Jurnal Fisika Unand (JFU)
Vol. 12, No. 4, Oktober 2023, hal. 666 – 673
ISSN: 2302-8491 (Print); 2686-2433 (Online)
https://doi.org/10.25077/jfu.12.4.666-673.2023

Open Access

Strain-Induced Control of Magnetic Anisotropy Energy in NbS_2 Monolayer: First-Principles Study

Berton Maruli Siahaan[1], Afrioni Roma Rio[1,*]
[1]Department of Physics, Faculty of Mathematics and Natural Sciences, Sam Ratulangi University, Manado, 95115, Indonesia

Article Info

Article History:
Diajukan: 15 April 2023
Direvisi: 20 Mei 2023
Diterima: 25 Juli 2023

Keywords:
Biaxial strain
Density functional theory
Magnetic anisotropy energy
NbS_2

Corresponding Author:
Afrioni Roma Rio
Email: afrioni@unsrat.ac.id

ABSTRACT

In this work, we investigate the strain controllability of magnetic anisotropy energy (MAE) in the monolayer form of niobium disulfide (NbS_2) using density functional theory (DFT). Our calculation reveals a negative MAE of -1.82 meV, indicating a preference for spins to align in the in-plane directions (x or y). By systematically applying biaxial tensile strain to the NbS_2 monolayer, ranging from 1% to 10%, we observe a linear relationship between strain and MAE. Interestingly, the strain-induced modulation of MAE leads to a remarkable phenomenon, where the easy axis of magnetization shifts from the in-plane to an out-of-plane orientation at a critical strain of 7%. This ability to switch the magnetic anisotropy by manipulating strain demonstrates the promising potential of NbS_2 monolayer in the development of spintronic devices.

I. INTRODUCTION

The successfully synthesis of graphene, a two-dimensional material, has sparked considerable interest in exploring other promising two-dimensional (2D) materials. This enthusiasm is driven by the attractive properties exhibited by graphene and the relatively straightforward exfoliation technique employed in its production. This interest extends to a class of materials called transition metal dichalcogenides (TMDs), which have garnered significant attention. TMDs encompass a range of compounds with a general formula of TX_2, where T represents a transition metal atom (such as Fe, Mo, Nb) and X denotes a chalcogen atom, including S, Se, or Te. A monolayer of 2D TMD consists of three atomics layers, with the transition metal (T) situated between two layers of chalcogen atoms (X) (Chhowalla *et al.*, 2015).

Over past decades, TMDs have been extensively studied both experimentally and theoretically due to their tremendous potential in technological applications. Computational material research, particularly employing density functional theory (DFT), has played a vital role in investigating the fundamental properties and controllable aspects of 2D materials (Bhimanapati *et al.*, 2015). Notably, voltage modulation of magnetic crystalline anisotropy (MCA) in TMD monolayers has been studied and reportedly that the magnetization orientation of certain monolayers can be switched under an electric field (Sui *et al.*, 2017). Additionally, external treatments such as strain and interfacial engineering have been reported to modify the physical properties of TMD materials (Ghorbani-Asl *et al.*, 2013; Li & Tang, 2020; Zhou *et al.*, 2012).

NbS_2 belongs to the family of layered materials, characterized by a hexagonal lattice structure comprising niobium (Nb) and sulfur (S) atoms. This structure gives rise to remarkable properties that make NbS_2 an attractive material for exploration. Some of the key characteristics of NbS_2 include its intrinsic superconductivity, excellent electrical conductivity, and the ability to undergo a phase transition under external stimuli as pressure and temperature. These attributes open up a multitude of possibilities for NbS_2-based devices and technologies (Wang *et al.*, 2020). In the study (Zhao *et al.*, 2016) which developed a straightforward chemical vapor deposition (CVD) method for the growth of few-layered NbS_2 (3R phase) directly on atomically flat hexagonal boron nitride (*h*BN) substrates, enabling the successful creation of 2D metallic TMDs with large single-domain sizes. This breakthrough provides a novel synthetic pathway for controlled growth of 2D metallic materials, facilitating the exploration of unique physics in 2D metals and the search for novel 2D superconductors. Subsequently, numerous studies have emerged, collectively demonstrating the promising potential of NbS_2 as highly favorable material for various applications (El Youbi *et al.*, 2021; Heil *et al.*, 2017; Najafi *et al.*, 2019; Shen *et al.*, 2022; van Loon *et al.*, 2018; Wang *et al.*, 2020; Zhang *et al.*, 2023).

In this study, we present a first-principles investigation of the magnetic properties of niobium disulfide (NbS_2) monolayer, one of the TMD materials. We begin providing an overview of the computational details, followed by a discussion of the material's physical properties. Finally, we present our conclusions.

II. COMPUTATIONAL METHOD

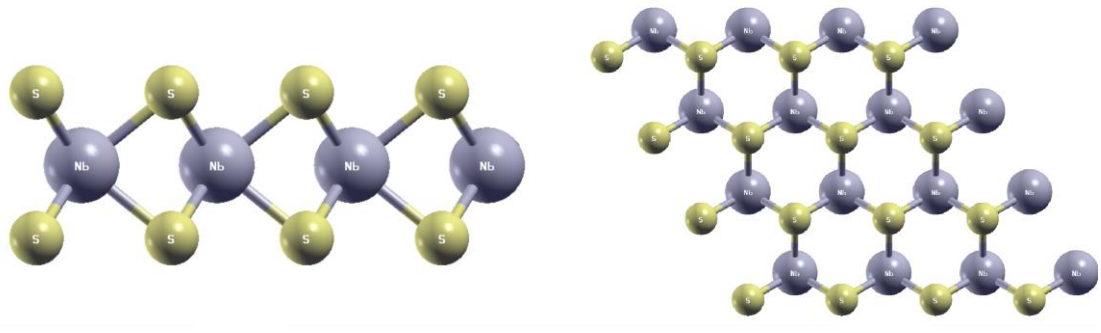

(a) (b)

Figure 1 Crystal structure of NbS_2 monolayer (a) side view, (b) top view

The niobium disulfide (NbS_2) monolayer adopts a layered hexagonal structure, as depicted in Figure 1. The unit cell consists of three atoms, S-Nb-S, with a lattice constant *a*. To avoid interlayer interactions, a vacuum region of 15 Å is introduced in the two perpendicular directions. Notably, previous studies on NbS_2 monolayers have recommended vacuum thicknesses of 10 Å (Heil *et al.*, 2018) and 15 Å (Sun *et al.*, 2018) to effectively prevent interlayer interactions. Therefore, based on this established research, we assert that a vacuum region of 15 Å is adequate to ensure the absence of interlayer interactions in our study. The Nb atom is positioned at (2/3 *a*, 1/3 *a*, ½ *c*), while the S atoms are located at the origin, separated from the Nb atom by approximately 1.56 Å in the z-direction (both above and below). It should be noted that the structure between the Nb and S atoms may undergo changes during geometry optimization and under applied strain.

For the first-principles calculations based on density functional theory (DFT) (Kohn & Sham, 1965), we employed the Quantum ESPRESSO code (Giannozzi *et al.*, 2009, 2017, 2020) within the generalized gradient approximation (GGA) using the Perdew, Burke, and Ernzerhof (PBE) exchange-correlation functional (Perdew *et al.*, 1996). Ultra-soft pseudopotentials with scalar relativistic pseudopotentials were used for noncollinear/spin-orbit coupling (SOC) calculations. These pseudopotentials were obtained from the PSlibrary (Dal Corso, 2014). To calculate the magnetic anisotropy energy (MAE), a noncollinear calculation was performed, where the MAE is defined as the difference in total energy between two magnetics states with magnetization aligned along in-plane ($E_{[100]}$) and out-of-plane ($E_{[001]}$) orientations, MAE = ($E_{[100]}$-$E_{[001]}$). In Quantum Espresso, to define the magnetization angle, two parameters, namely `angle1` and `angle2`, can be utilized. The `angle1` parameter represents the angle in degrees between the initial magnetization and the z-axis, while `angle2` represents the angle in degrees between the projection of the initial magnetization onto the x-y plane and the x-axis. For the in-plane direction ($E_{[100]}$), the angles can be set as follows: `angle1` = 90 degrees and `angle2` = 0 degrees. Conversely, for the out-of-plane direction ($E_{[001]}$), the angles should be set as follows: `angle1` = 0 degrees and `angle2` = 0 degrees. These angle settings enable us to accurately define the desired magnetic orientations and subsequently calculate the corresponding MAE values for our study.

The kinetic energy cutoff for the wavefunctions was set to 50 Ry, which was optimized (refer to Appendix Figure A.1). The *k*-point mesh was also optimized (refer to Appendix Figure A.1), and an $8 \times 8 \times 1$ *k*-point grid was employed for ionic minimization with a convergence threshold on forces smaller than 0.0001 Ry/Bohr. For electronic structural optimization, a $12 \times 12 \times 1$ *k*-point grid was utilized to achieve higher accuracy. Biaxial strain ranging from 1% to 10% was applied along the desired directions by varying the lattice constants. For example, if the initial lattice constant a_0 is 3.34 Å, a 1% tensile strain would result in a new lattice constant of $a_0 + \left(\frac{1}{100} \times a_0\right)$, which equals 3.38 Å. This process continues for each incremental strain level, up to 10%. The MAE is then calculated for each applied strain.

III. RESULTS AND DISCUSSION

In our study, we initially determined the optimum lattice constant a_0 of the NbS_2 monolayer, where the energy is minimized. Figure 2 shows that using the Birch-Murnaghan equation of state (Birch, 1947), the calculated a_0 for NbS_2 is 3.34 Å, which consistent with previous findings (Bianco *et al.*, 2019; Güller *et al.*, 2012; Stan *et al.*, 2019; Sun *et al.*, 2018; Zhou *et al.*, 2012). Upon applying biaxial tensile strain to the NbS_2 monolayer, the lattice constant *a* increases, resulting in a decrease in the distance between the chalcogen atoms S ($l_{S\text{-}S}$), and an increase in the bond length the Nb and S atoms ($l_{Nb\text{-}S}$) (see Table 1).

Our calculations for the optimized structural geometry of the NbS_2 monolayer align closely with a previous study (Zhou *et al.*, 2012). We observed that even at a tensile strain of 10%, the change in the Nb-S bond length ($l_{Nb\text{-}S}$) was only 4% compared to the unstrained structure. For S-S bond length ($l_{S\text{-}S}$), the change was also relatively small, at just 5%. This relatively small variation indicates the material's elastic tolerance, suggesting that it can withstand significant strain without undergoing structural breakdown. This characteristic implies the potential for precise control over the electronic and magnetic properties of NbS_2.

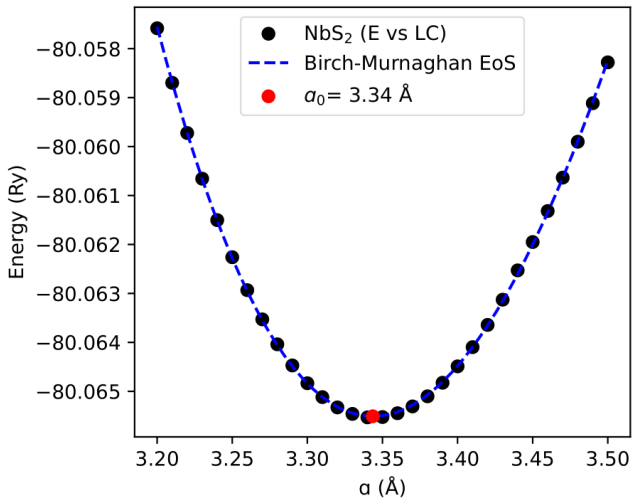

Figure 2 Lattice constant optimization using Birch-Murnaghan equation of state

Moving on to the electronic and magnetic properties, the electronics states depicted in Figure 3 reveal that the valence band and conduction band overlap near the Fermi level, indicating that the NbS_2 monolayer behaves as a metal. The magnetic character originates from the Nb atom, with a magnetic moment of 0.20 µB at 0% strain, which doubles starting from 5% (see Table 1). In light of previous research, it is worth noting that the magnetic moment of the material can be significantly enhanced by the application of tensile strain, as demonstrated by (Zhou *et al.*, 2012). Furthermore, findings from a separate study by (Sui *et al.*, 2017) indicate a positive correlation MAE and the magnetic moment, suggesting that an increase in MAE can also result in an increase in the magnetic moment.

Table 1 NbS_2 structure and magnetic properties (lattice constant, a; distance between chalcogen atoms S-S, $l_{S\text{-}S}$; bond length of Nb-S, $l_{Nb\text{-}S}$; magnetic moment for Nb atom in Bohr magneton, M_{Nb}) with respect to strain.

	biaxial tensile strain										
	0%	1%	2%	3%	4%	5%	6%	7%	8%	9%	10%
a (Å)	3.34	3.38	3.41	3.44	3.48	3.51	3.54	3.58	3.61	3.64	3.68
$l_{S\text{-}S}$ (Å)	3.13	3.11	3.08	3.08	3.06	3.04	3.02	3.01	2.99	2.98	2.96
$l_{Nb\text{-}S}$ (Å)	2.48	2.49	2.51	2.51	2.52	2.53	2.54	2.55	2.57	2.58	2.59
M_{Nb} (µB)	0.20	0.21	0.22	0.22	0.22	0.43	0.44	0.45	0.46	0.46	0.47

We chose to focus on four specific variations of strain in the PDOS calculation, namely 0% strain, 2% strain, 4% strain, and 7% strain, because they were deemed representative enough to effectively demonstrate the relationship between strain and MAE (Figure 3). The observed trends in MAE at these specific strain levels provided clear insights into how MAE changes with strain, particularly highlighting a significant shift in MAE occurring around 7% strain.

Next, we focused on the determining the magnetic anisotropy energy (MAE) of the NbS_2 monolayer in response to biaxial tensile strain. The results are illustrated in Figure 4. The unstrained NbS_2 monolayer exhibits an MAE of -1.82 meV, where negative values indicate a preference for spins to align in the in-plane direction. As the monolayer is subjected to tensile strain, the MAE linearly increases and transitions to the out-of-plane direction at 7%. We do not have direct reference data for our strain-induced MAE results. However, previous study on TMDs found that MAE favors an in-plane orientation with negative values (Sui *et al.*, 2017). Notably, our unstrained condition also exhibits negative MAE values, aligning with Sui's findings and lending support to our results within the broader context of TMDs' magnetic anisotropy.

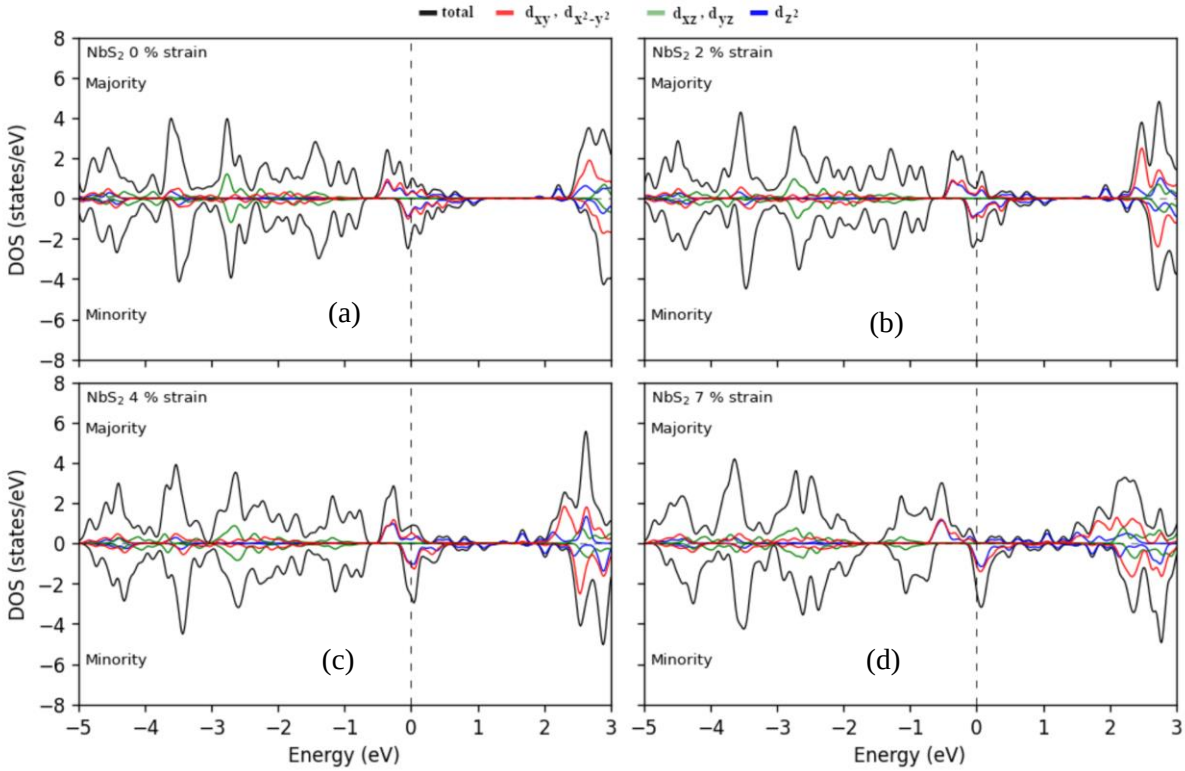

Figure 3 Projected density of states (PDOS) of NbS_2 monolayer, (a) 0% strain, (b) 2% strain, (c) 4% strain and (d) 7% strain. The black lines show the total density of states, whereas the red, green, and blue lines represent the density of Nb *d* orbital states. The Fermi level is represented by the vertical dashed lines.

To explain the switching of MAE, we introduce the spin-orbit coupling (SOC) as a perturbation term in the Hamiltonian. The MAE can be expressed in terms of the coupling between occupied and unoccupied states through the orbital angular momentum operators $\hat{\boldsymbol{L}}_{\boldsymbol{z}}$ and $\hat{\boldsymbol{L}}_{\boldsymbol{x}}$, as well as the energy difference between these states (Sui *et al.*, 2017):

$$MAE = \xi^2 \sum_{o,u} \frac{\left|\left(\psi_o^{\uparrow(\downarrow)}\middle|\hat{L}_z\middle|\psi_u^{\uparrow(\downarrow)}\right) - \left(\psi_o^{\uparrow(\downarrow)}\middle|\hat{L}_x\middle|\psi_u^{\uparrow(\downarrow)}\right)\right|^2}{E_u^{\uparrow(\downarrow)} - E_o^{\uparrow(\downarrow)}} + \underbrace{\frac{\left|\left(\psi_o^{\uparrow(\downarrow)}\middle|\hat{L}_x\middle|\psi_u^{\uparrow(\downarrow)}\right) - \left(\psi_o^{\uparrow(\downarrow)}\middle|\hat{L}_z\middle|\psi_u^{\uparrow(\downarrow)}\right)\right|^2}{E_u^{\uparrow(\downarrow)} - E_o^{\uparrow(\downarrow)}}}_{spin-flipterm} \qquad (1)$$

where ξ represent the SOC constant, $\psi_o^{\uparrow(\downarrow)}$ and $\psi_u^{\uparrow(\downarrow)}$ denote the occupied and unoccupied majority-spin (minority-spin) states, and $E_o^{\uparrow(\downarrow)}$ and $E_u^{\uparrow(\downarrow)}$ are the respective energies.

In terms of *d* orbitals, the magnetic quantum number *m* splits into three groups: $|m| = 0(d_{z^2})$, $|m| = 1\ (d_{xz}, d_{yz})$, and $|m| = 2\ (d_{xy}, d_{x^2-y^2})$. The first term in Equation 1 represents the coupling states with the same spin (e.g., majority to majority). SOC between occupied and unoccupied states with the same *m* through the $\hat{L}_z$ operator contributes positively to the MAE. Conversely, SOC between occupied and unoccupied states with different *m* through the $\hat{L}_x$ operator contributes negatively to the MAE. The second term, known as the spin flip term, contributes to the MAE in the opposite manner.

In the case of the NbS_2 monolayer at zero strain, the coupling between occupied (below the Fermi level) and unoccupied states (above the Fermi level) through the $\hat{L}_x$ operator for the majority spin with different magnetic quantum numbers, $|m| = 0$ (blue lines) and $|m| = 2$ (red lines), leads to a negative contribution to the MAE. This negative contribution is also observed for the minority spin.

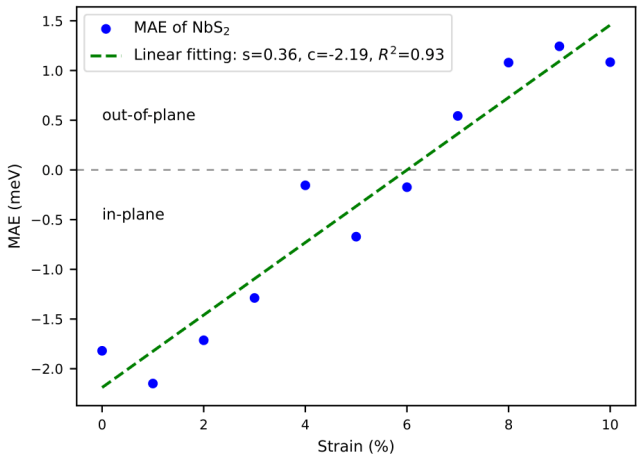

Figure 4 Magnetic anisotropy energy (MAE) of NbS_2 monolayer with respect to strain. The dashed line is curve fitting using linear regression, with slope (s), intercept (c), and coefficient of determination (R^2).

As biaxial tensile strain is applied to the NbS_2 monolayer, the *d* orbitals of the Nb atom shift to the occupied for the majority spin, resulting in a significant reduction in the proportion of *d* orbitals near the Fermi level. When the strain reaches 7%, the *d* states are nearly eliminated around the Fermi level, leading to a substantial decrease in the negative contribution to the MAE. Similarly, the *d* orbitals of the minority spin shift to the unoccupied state, further reducing the negative contribution to the MAE. In the case of PDOS at 5% strain, we observed that the *d* states are indeed nearly eliminated around the Fermi level. However, it is important to note that despite this change, the coupling of the spin-split term is not substantial enough to significantly alter the MAE. As a result, the MAE still favors the in-plane orientation.

Taking into account the second term of the equation (spin-flip term), the coupling between occupied states of the minority spin and unoccupied states of the majority spin, or vice versa, with different magnetic quantum numbers $|\boldsymbol{m}| = \mathbf{0}$ (blue lines) and $|\boldsymbol{m}| = \mathbf{2}$ (red lines) through the $\hat{\boldsymbol{L}}_{\boldsymbol{x}}$ operator, yields a positive contribution to the MAE. Consequently, as the strain increases, the negative terms contribute less to the MAE, while the positive terms contribute more, resulting in a shift of the MAE from negative to positive.

IV. CONCLUSION

In this study, we employed density functional theory and first-principles calculations to examine the magnetic anisotropy energy (MAE) of layered NbS_2 under biaxial tensile strain. Our findings provide valuable insights into the behavior and potential applications of NbS_2 monolayers.

Our results demonstrate that the NbS_2 monolayer exhibits metallic behavior, with the magnetic properties originating from the Nb atoms. We observed that applying tensile strain to the monolayer induces changes in the Nb-S bond length ($l_{\text{Nb-S}}$) of up to 4%, while maintaining elastic tolerance and avoiding structural breakdown. This suggests the feasibility of precise control over the electronic and magnetic properties of NbS_2 through strain engineering.

Notably, we discovered a significant phenomenon: at a strain of 7%, the orientation of the MAE can be switched from an in-plane direction to a perpendicular direction. This finding holds promising potential for the development of spintronics devices, where the ability to manipulate and switch the MAE is of great importance.

Our study contributes to the understanding of the underlying mechanisms governing the electronic and magnetic properties of NbS_2 monolayers under strain. However, there are still avenues for further exploration. Future investigations could explore alternative strain engineering approaches, such as uniaxial strain or strain gradients, to uncover additional means of controlling the electronic and magnetic behavior of NbS_2. Additionally, the influence of external factors, including temperature and defects, on the properties of NbS_2 monolayers could be investigated to broaden our understanding and pave the way for practical applications.

In conclusion, our comprehensive analysis of the MAE in strained NbS_2 monolayers sheds light on the potential of these materials for spintronic devices. The ability to modulate and switch the MAE orientation open up**s** exciting opportunities for future technological advancements in the field of spintronics.

APPENDIX A. SUPPLEMENTARY DATA

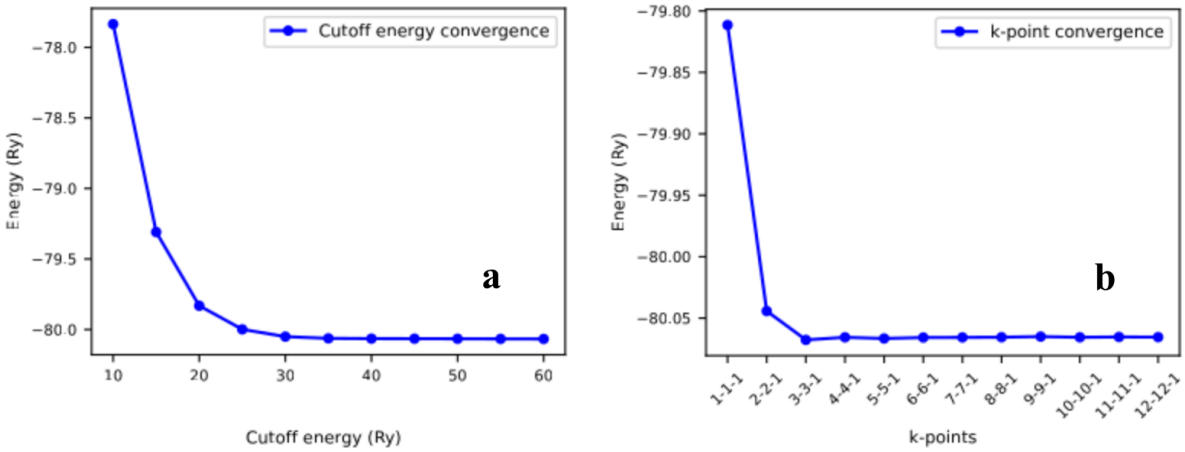

Figure A.1 NbS_2 monolayer convergence tests, (a) cutoff energy convergence, (b) *k*-points convergence

REFERENCE

Bhimanapati, G. R., Lin, Z., Meunier, V., Jung, Y., Cha, J., Das, S., Xiao, D., Son, Y., Strano, M. S., Cooper, V. R., & others. (2015). Recent advances in two-dimensional materials beyond graphene. *ACS Nano*, *9*(12), 11509–11539.

Bianco, R., Errea, I., Monacelli, L., Calandra, M., & Mauri, F. (2019). Quantum enhancement of charge density wave in NbS2 in the two-dimensional limit. *Nano Letters*, *19*(5), 3098–3103.

Birch, F. (1947). Finite elastic strain of cubic crystals. *Physical Review*, *71*(11), 809.

Chhowalla, M., Liu, Z., & Zhang, H. (2015). Two-dimensional transition metal dichalcogenide (TMD) nanosheets. *Chemical Society Reviews*, *44*(9), 2584–2586.

Dal Corso, A. (2014). Pseudopotentials periodic table: From H to Pu. *Computational Materials Science*, *95*, 337–350.

El Youbi, Z., Jung, S. W., Richter, C., Hricovini, K., Cacho, C., & Watson, M. D. (2021). Fermiology and electron-phonon coupling in the 2 H and 3 R polytypes of Nb S 2. *Physical Review B*, *103*(15), 155105.

Ghorbani-Asl, M., Borini, S., Kuc, A., & Heine, T. (2013). Strain-dependent modulation of conductivity in single-layer transition-metal dichalcogenides. *Physical Review B*, *87*(23), 235434.

Giannozzi, P., Andreussi, O., Brumme, T., Bunau, O., Nardelli, M. B., Calandra, M., Car, R., Cavazzoni, C., Ceresoli, D., Cococcioni, M., & others. (2017). Advanced capabilities for materials modelling with Quantum ESPRESSO. *Journal of Physics: Condensed Matter*, *29*(46), 465901.

Giannozzi, P., Baroni, S., Bonini, N., Calandra, M., Car, R., Cavazzoni, C., Ceresoli, D., Chiarotti, G. L., Cococcioni, M., Dabo, I., & others. (2009). QUANTUM ESPRESSO: a modular and open-source software project for quantum simulations of materials. *Journal of Physics: Condensed Matter*, *21*(39), 395502.

Giannozzi, P., Baseggio, O., Bonfà, P., Brunato, D., Car, R., Carnimeo, I., Cavazzoni, C., De Gironcoli, S., Delugas, P., Ferrari Ruffino, F., & others. (2020). Quantum ESPRESSO toward the exascale. *The Journal of Chemical Physics*, *152*(15), 154105.

Güller, F., Helman, C., & Llois, A. (2012). Electronic structure and properties of NbS2 and TiS2 low dimensional structures. *Physica B: Condensed Matter*, *407*(16), 3188–3191.

Heil, C., Poncé, S., Lambert, H., Schlipf, M., Margine, E. R., & Giustino, F. (2017). Origin of superconductivity and latent charge density wave in NbS 2. *Physical Review Letters*, *119*(8), 087003.

Heil, C., Schlipf, M., & Giustino, F. (2018). Quasiparticle G W band structures and Fermi surfaces of bulk and monolayer NbS 2. *Physical Review B*, *98*(7), 075120.

Kohn, W., & Sham, L. J. (1965). Self-consistent equations including exchange and correlation effects. *Physical Review*, *140*(4A), A1133.

Li, F., & Tang, Q. (2020). Modulating the electronic structure and in-plane activity of two-dimensional transition metal dichalcogenide (MoS2, TaS2, NbS2) monolayers by interfacial engineering. *The Journal of Physical Chemistry C*, *124*(16), 8822–8833.

Najafi, L., Bellani, S., Oropesa-Nuñez, R., Martín-García, B., Prato, M., Mazánek, V., Debellis, D., Lauciello, S., Brescia, R., Sofer, Z., & others. (2019). Niobium disulphide (NbS 2)-based (heterogeneous) electrocatalysts for an efficient hydrogen evolution reaction. *Journal of Materials Chemistry A*, *7*(44), 25593–25608.

Perdew, J. P., Burke, K., & Ernzerhof, M. (1996). Generalized gradient approximation made simple. *Physical Review Letters*, *77*(18), 3865.

Shen, W., Qiao, L., Ding, J., & Sui, Y. (2022). P and Se-codopants triggered basal plane active sites in NbS2 3D nanosheets toward electrocatalytic hydrogen evolution. *Applied Surface Science*, *581*, 152419.

Stan, R.-M., Mahatha, S. K., Bianchi, M., Sanders, C. E., Curcio, D., Hofmann, P., & Miwa, J. A. (2019). Epitaxial single-layer NbS 2 on Au (111): Synthesis, structure, and electronic properties. *Physical Review Materials*, *3*(4), 044003.

Sui, X., Hu, T., Wang, J., Gu, B. L., Duan, W., & Miao, M. S. (2017). Voltage-controllable colossal magnetocrystalline anisotropy in single-layer transition metal dichalcogenides. *Physical Review B*, *96*(4), 041410.

Sun, Y., Zhuo, Z., & Wu, X. (2018). Bipolar magnetism in a two-dimensional NbS 2 semiconductor with high Curie temperature. *Journal of Materials Chemistry C*, *6*(42), 11401–11406.

van Loon, E. G., Rösner, M., Schönhoff, G., Katsnelson, M. I., & Wehling, T. O. (2018). Competing Coulomb and electron–phonon interactions in NbS2. *Npj Quantum Materials*, *3*(1), 32.

Wang, W., Lei, W., Zheng, X., Li, H., Tang, X., & Ming, X. (2020). Electronic structure and phase transition engineering in NbS2: Crucial role of van der Waals interactions. *Chinese Physics B*, *29*(5), 056201.

Zhang, X., Zhou, X., Wang, Y., & Li, Y. (2023). A theoretical study of the NbS 2 monolayer as a promising anchoring material for lithium–sulfur batteries. *Physical Chemistry Chemical Physics*, *25*(14), 10097–10102.

Zhao, S., Hotta, T., Koretsune, T., Watanabe, K., Taniguchi, T., Sugawara, K., Takahashi, T., Shinohara, H., & Kitaura, R. (2016). Two-dimensional metallic NbS2: Growth, optical identification and transport properties. *2D Materials*, *3*(2), 025027. https://doi.org/10.1088/2053-1583/3/2/025027

Zhou, Y., Wang, Z., Yang, P., Zu, X., Yang, L., Sun, X., & Gao, F. (2012). Tensile strain switched ferromagnetism in layered NbS2 and NbSe2. *Acs Nano*, *6*(11), 9727–9736.